Tung, W.; Wang, W.; Liu, Y.; Gould, O.; Kratz, K.; Ma, N.; Lendlein, A.:
Mechanical characterization of electrospun polyesteretherurethane (PEEU) meshes by atomic force microscopy.
In: Clinical Hemorheology and Microcirculation. Vol. 73 (2019) 229 - 236.
First published online by IOS: November 13, 2019

DOI: 10.3233/CH-199201
https://doi.org/10.3233/CH-199201

Mechanical Characterization of Electrospun Polyesteretherurethane (PEEU) Meshes by Atomic Force Microscopy

Wing Tai Tung[1,2], Weiwei Wang[1], Yue Liu[1], Oliver E. C. Gould[1], Karl Kratz[1], Nan Ma[1, 3]*, Andreas Lendlein[1, 2, 3]*

[1] Institute of Biomaterial Science and Berlin-Brandenburg Centre for Regenerative Therapies, Helmholtz-Zentrum Geesthacht, Kantstrasse 55, 14513 Teltow, Germany

[2] Institute of Chemistry, University of Potsdam, Karl-Liebknecht-Str. 24/25, 14476 Potsdam, Germany

[3] Institute of Chemistry and Biochemistry, Free University of Berlin, 14195 Berlin, Germany

* To whom correspondence should be addressed: Prof. Dr. Nan Ma, Prof. Dr. Andreas Lendlein, Email: nan.ma@hzg.de, andreas.lendlein@hzg.de

Abstract

The mechanical properties of electrospun fiber meshes typically are measured by tensile testing at the macro-scale without precisely addressing the spatial scale of living cells and their submicron architecture. Atomic force microscopy (AFM) enables the examination of the nano- and micro-mechanical properties of the fibers with potential to correlate the structural mechanical properties across length scales with composition and functional behavior. In this study, a polyesteretherurethane (PEEU) polymer containing poly(*p*-dioxanone) (PPDO) and poly(*ε*-caprolactone) (PCL) segments was electrospun into fiber meshes or suspended single fibers. We employed AFM three point bending testing and AFM force mapping to measure the elastic modulus and stiffness of individual micro/nanofiber and the fiber mesh. The local stiffness of the fiber mesh including the randomized, intersecting structure was also examined for each individual fiber. Force mapping results with a set point of 50nN demonstrated the dependence of the elasticity of a single fiber on the fiber mesh architecture. The non-homogeneous stiffness along the same fiber was attributed to the intersecting structure of the supporting mesh morphology. The same fiber measured at a point with and without axial fiber support showed a remarkable difference in stiffness, ranging from 0.2 to 10 nN/nm respectively. For the region, where supporting fibers densely intersected, the stiffness was found to be considerably higher. In the region where the degrees of freedom of the fibers was not restricted, allowing greater displacement, the stiffness was observed to be lower. This study elucidates the relationship between architecture and the mechanical properties of a micro/nanofiber mesh. By providing a greater understanding of the role of spatial arrangement and organization on the surface mechanical properties of such materials,

we hope to provide insight into the design of microenvironments capable of regulating cell functionality.

Keywords: Biomaterials, AFM, Electrospinning, Elastic modulus, Force mapping

Introduction

The extracellular matrix (ECM) is a complex 3D microenvironment providing both chemical and physical cues to the cells and subsequently instructing cellular function[1]. Physical cues are of great interest because structural mechanical properties including stiffness and tension loading regulate cell spreading[2,3], cell cycle[4], and play an important role in stem cells´ fate commitment[5–9]. These mechanical cues are mainly provided by ECM fibers which are naturally organized in the ECM meshwork, such as collagen and elastin, in an aligned or networked arrangement[10]. In contrast to a bulk material substrate possessing homogeneous properties, the mechanical properties and functionality of a fiber mesh substrate is highly dependent on the morphology and architecture of the fiber mesh. A variation in fiber diameter, density, porosity and orientation all contribute to the inhomogeneity of the ECM. The substrate stiffness is a product of the combination of material stiffness and geometry[11], where the organization of the fibers plays an important role in determining the stiffness felt by the cells[12].

Previous work has demonstrated that in randomly orientated fiber networks in aqueous environments, the partially suspended nature of intersecting hydrogel fibers allowed higher fiber mobility, allowing attached cells to displace the fibers and enhancing cellular functionality[13]. Furthermore, in a weld (intersection point jointed) fiber network, cells displaced the free suspended portion of these fibers[13]. Such fibrous scaffolds enable a higher amount of matrix architecture modification by cells when compared to a conventional 2D plane surface substrate. This is facilitated by the extra degrees of freedom afforded to fibers suspended in such electrospun meshes, enabling local deformation which is impossible in continuous bulk materials.

In order to evaluate the mechanical properties of fiber-based substrates, typically macroscopic tensile testing is performed[14]. In such testing, a uniaxial force applied to meshes containing randomly orientated fibers causes the re-orientation of fibers in the

direction of applied load, leading to a decrease in mesh cross-sectional area below 5% strain[15,16]. While tensile testing has proved to be an effective tool for the mechanical characterization of electrospun fiber meshes at the macro-scale, the spatial scale of cell sensing[16] means that micro-scale characterization of fiber meshes is needed to enable their use as cell culture substrates. This difference in scale has greatly hindered the relation of material properties to cell behavior.

AFM-based three-point bending tests on single fibers (Fig. 1), employing the Euler-Bernoulli double-clamped beam equation (eqn 1), have been demonstrated to be a suitable method to determine a fiber's elastic modulus with high accuracy[17,18]. In such testing, a vertically applied force causes small deflections of fibers in the linear elastic regime, allowing for the determination of the axial or bending elastic modulus[19,20]. However, the fibrous scaffold is not presented as a single fiber to cells, but a collection of fibers in a meshwork[10], where the overlap and intersection of fibers form a complex network. In addition to mechanical properties of a single fiber, the mechanical properties considered in terms of the meshwork is of interest as this provides insight into cell's interpretation of the ECM during morphological change of ECM by cells[13,21]. AFM based force mapping can provide an overview of mechanical properties over an area of interest, like the ratio of F(x)/d can be interpreted as the fiber's stiffness at each deformation position on the force map[22]. The usage of AFM force mapping of fibrous scaffold to relate the architecture and relevant stiffness is currently unexplored.

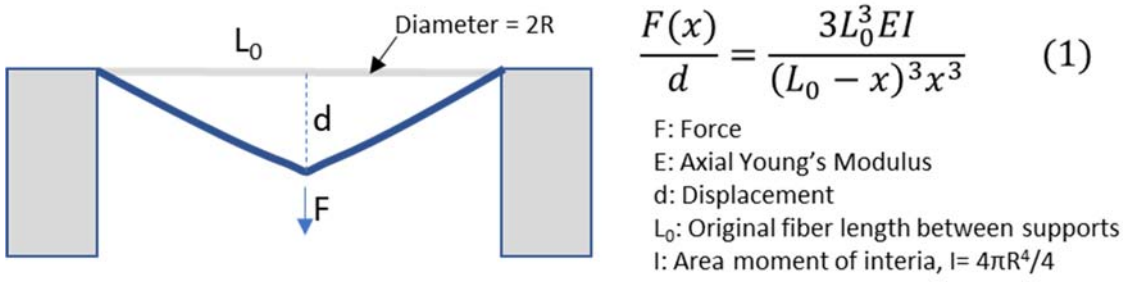

$$\frac{F(x)}{d} = \frac{3L_0^3 EI}{(L_0 - x)^3 x^3} \qquad (1)$$

F: Force
E: Axial Young's Modulus
d: Displacement
L_0: Original fiber length between supports
I: Area moment of interia, $I = 4\pi R^4/4$

Figure 1. Illustration of AFM-based measurement in characterizing mechanical properties of fibers. Force vs. displacement on the fiber during three point bending measurement is calculated from an equation derived for the double-clamped beam model.

We hypothesize that the complex organization of the fiber meshwork, consisting of intersecting and suspended microfibers shows a variation in surface mechanical

properties related to the architectural organization of the fibers. In this study a polyesteretherurethane (PEEU) containing poly(*p*-dioxanone) (PPDO) and poly(*ε*-caprolactone) (PCL) in a weight ratio of 50:50 was electrospun into fiber meshes. In addition to the AFM-based three-point bending tests, AFM-based force mapping was used to map the mechanical properties of the fiber meshes. These experiments aimed to combine the mechanical properties of single fibers with the effect of architecture of the meshwork, yielding insight into the mechanical cues communicated to cells during culture.

Method and materials

Chemical and reagents

Polyesteretherurethane (PEEU) polymer was prepared as previously described[23] from L-lysine diisocyanate as the linker for poly(*p*-dioxanone) diol (PPDO) and poly(*ε*-caprolactone) diol (PCL). The PPDO and PCL weight ratio is 50:50 (abbreviated as PEEU50) with a molecular weight of 79,000g/mol as measured by gel permeation chromatography (GPC).

Hexafluoroisopropanol (HFIP), which was used as a solvent for PEEU during electrospinning was purchased from Abcr GmbH (AB102635). The UV glue (Vitralit 7283) for fixing the PEEU fibers on silicon structure was purchased from Panacol-Elosol GmbH.

Preparation of electrospun fibers

The electrospinning setup (Linari Engineering, Italy) included the voltage supply, rotatory drum collector, and two syringe pumps. The electrospinning process was performed inside of a home-made transparent plastic chamber with tubing connected to air source for humidity control. PEEU50 was dissolved in HFIP at a concentration of 17 wt%. The polymer solution was filtered with glass fiber syringe filter with pore size of 1 μm before electrospinning. A 9-gauge blunt tip needle was used for electrospinning. The flowrate of PEEU50 solution supply during electrospinning was 1.77 ml/hr, with a tip to collector distance of 25 cm. The voltage supply for stable electrospinning was 10-15 kV at an environmental humidity of 20%. The PEEU50 fiber mesh sample was prepared by electrospinning onto a drum collector rotating at 5 rpm

for 2 hours, producing a mesh thickness of 48 µm. A single fiber was collected on a microstructured silicon substrate coated in a UV adhesive and fixed on rotating drum collector for 4 rotations, followed by 30 minutes of UV exposure for fixation.

Atomic force microscopy (AFM) measurement

AFM measurement was performed on a BioAFM Nanowizard (JPK BioAFM). A OMCL-AC200TS cantilever from Olympus was used (spring constant 9 N/m). At the beginning of each measurement the sample was first imaged in AC mode before force measurements were carried out in contact mode. Force microscopy measurements were performed by addressing a series of points along the length of the fiber for the three point bending measurements, or for force mapping with a grid size of 30 x 30 µm, with 128 x 128 points. Force set points used of 50 nN, 100 nN, 200 nN and 500 nN were used in the three point bending tests. The force set point used for force mapping was 50 nN. The data processing software of the BioAFM Nanowizard was used for analysis.

Results and Discussion

AFM Three-point Bending Tests

To perform a three-point bending test, a chosen fiber fixed between two silicon square pillars was imaged with AC mode, enabling the fiber to be accurately addressed during the force spectroscopy measurement. Figure 2a shows the measured height image of a representative fiber. For clearer visualization of the scanned fiber, the lock-in amplitude image (Fig. 2b) was used for locating the fibers. The diameter of the scanned fibers was measured as 0.9 ± 0.2 µm. A series of points along the middle of a scanned fiber was chosen for the force measurement (white dots, Fig. 2b). Four different force set point values, 50 nN, 100 nN, 200 nN, 500nN were used for the measurement. By using the Euler-Bernoulli double-clamped beam model, the corresponding elastic modulus at a defined position and force value could be obtained by fitting the curve of stiffness $\frac{F(x)}{d}$ vs. position with the model. As a result, the axial E modulus was calculated as 200 ± 45 MPa. The stiffness profile (Fig. 2c) showed a variation with position on the fiber, with higher values observed at locations towards

the fixed end points and lower values at the midpoint. This is in agreement with measurements reported elsewhere[20].

The stiffness decreased from 10 ± 1 nN/nm to 0.2 ± 0.03 nN/nm when moving the contact point from the edge to the midpoint along the suspended fiber between two fixed supports. Therefore, the 3D arrangement of the underlying fiber support and contact position has a significant influence on the stiffness of the fibers. We expect this finding to provide insight into the physical properties of the fiber mesh substrate.

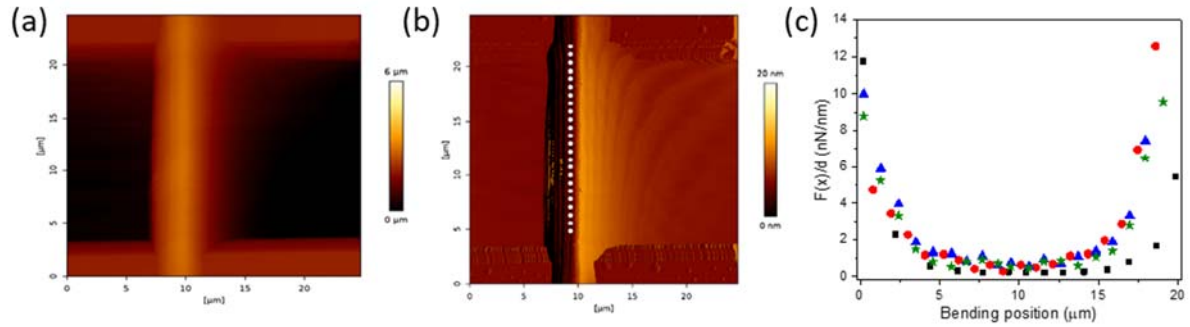

Figure 2. AFM measurement on single fiber suspended between pillars. (a) AFM height image of a single PEEU fiber supported on structured silicon wafer with spacing of 20 µm. (b) AFM amplitude image with numbered position of test points along the suspended fiber. (c) Slope F(x)/d of force-distance curve as a function of the bending position along the suspended fiber with different loadings of 50 nN (black square), 100 nN (red circle), 200 nN (blue triangle) and 500 nN (green star).

AFM Force Mapping

To investigate the local mechanical properties of the fiber mesh, force mapping was used to characterize the fiber mesh sample. A 30 x 30 µm^2 area was chosen for the mapping with a grid size of 128 x 128 at a set point of 50 nN. From the measured height image (Fig. 3a) and 3D projection (Fig. 3b), the surface arrangement of the fibers could be examined. The processed force curves were used to create the stiffness map (Fig. 3c), and displacement map (Fig. 3d).

Comparing these images with the 3D projection of the height image, indicates that the deviation in the stiffness and displacement maps can be explained in terms of the support provided by the underlying fiber network. This is likely a result of the mobility of the suspended fibers. From the displacement map (Fig. 3d), the majority of the uppermost fiber layer were displaced to a maximum of 20 nm under a force of 50 nN,

but certain portions of the suspended fibers were displaced to 100 nm or more under the same force. The suspended fibers that did not show a similar phenomenon are likely supported by fibers that the vertically displaced cantilever cannot reach and image. The further development of *in-situ* 3D tomography and AFM techniques would greatly aid research in this area.

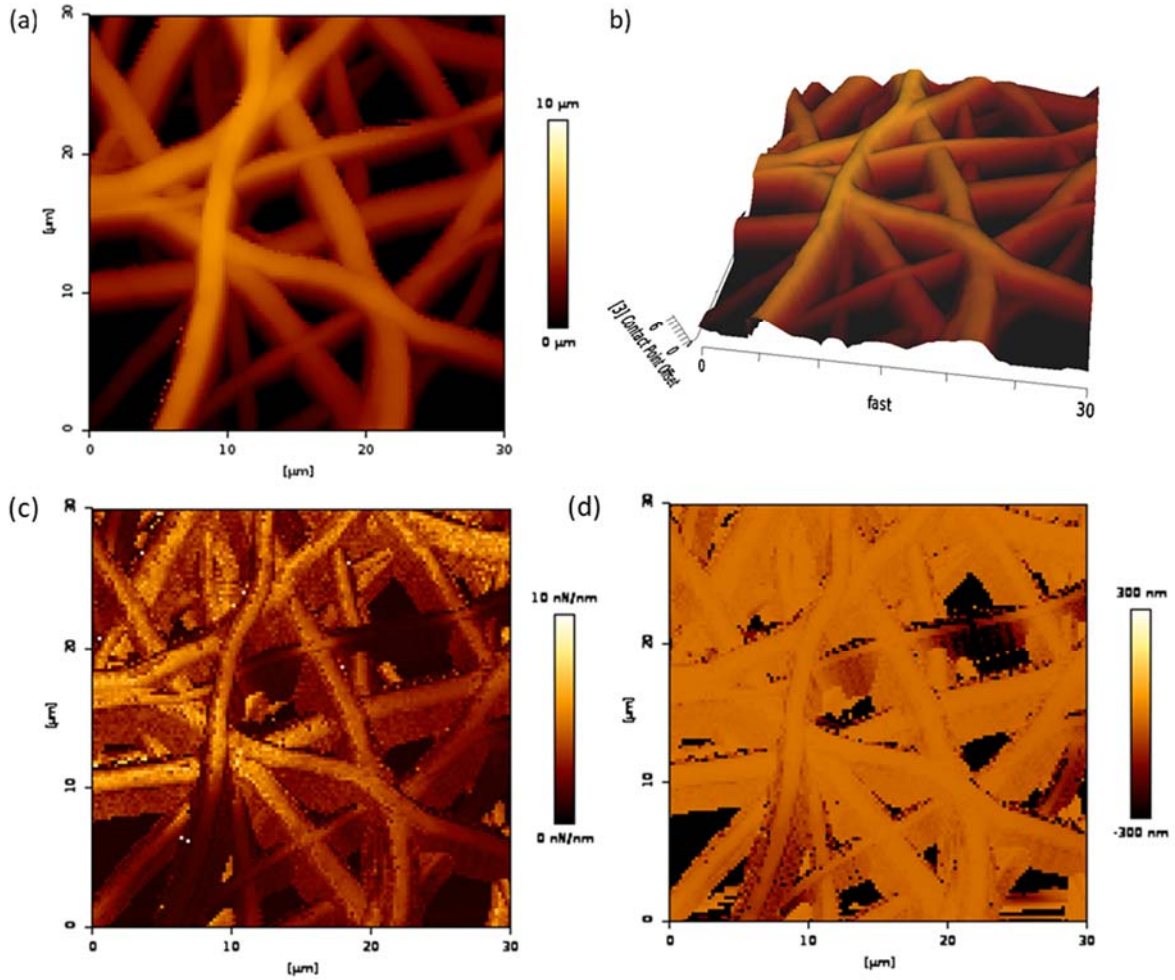

Figure 3. AFM based force mapping of fiber meshwork. (a) Height information of the fiber mesh topography extracted from the contact point offset of the force map. (b) 3D representation of the fiber mesh height information. (c) slope F(x)/d from force-distance curves of the force map (d) The displacement from the contact point at set force of 50nN of the force map.

For regions where fibers were densely intersecting, the stiffness was higher as the underlying fibers restricted their vertical displacement. The difference in stiffness of the fibers between the suspended portion and the intersecting portion can be more than five times. For suspended fibers below the immediate surface, the stiffness of suspended portions was in the range of 0.2 ± 0.02 nN/nm as opposed to the supported

regions, which showed values of 5 ± 1 nN/nm. A major limitation of this technique is its inability to provide structural information below the first few layers of fibers. Fibers supporting the suspended fiber not reached by the AFM cantilever during imaging, could be influencing the stiffness and displacement.

The surface of the fiber network could be conceptualized as a collection of individual points that define the fiber network structure and architecture on a substrate. Previous work has elegantly visualized this by varying the height of PDMS pillar arrays, enabling the variation of the local stiffness of a microstructured surface used for cell attachment[24]. After placement on the surface, the cells express integrin, subsequently providing links to each point[25]. Pushing or pulling on any of the points will result in the cell experiencing the local mechanical properties of the substrate. When this mechanical signal is transduced into the cell through integrin and focal adhesion[26], the talin in focal adhesion acts as a mediator in response to the force and induced focal adhesion maturation[27–29]. This results in the stabilizing of cytoskeleton for mechanotransduction to the nucleus[30]. Because talin responses directly to the ECM's mechanical properties, the stiffness map generated by AFM force mapping can be interpreted as how the cell's focal adhesion translates the ECM mechanical properties, subsequently transducing the information to the nucleus that results in cellular functionality.

While AFM mapping is limited to the vertical displacement of the fibers, the cell mediated movement of fibers also includes lateral displacement. Despite this limitation, measurements obtained by vertical displacement should provide a measure of the general mobility of a fiber in a fibrous scaffold.

Conclusion

AFM based force mapping were used to elucidate the local mechanical properties of a microfiber meshwork in order to determine their dependency on the microscale network architecture. In contrast to conventional macroscale tensile testing, AFM based three point bending tests or force mapping enabled the characterization of single fibers and enabled their comparison to the local fiber meshwork. Here, by mapping the slope from force curves of a section of fiber mesh we observed that the stiffness is highly dependent on the supporting architecture of the fiber, where

intersecting points showed a higher stiffness when compared to suspended sections. This work provides a model to understand the mechanical properties of natural ECM fiber meshworks, and the role of architecture in influencing cell behavior. Further work is required to obtain multidirectional information about the physical behavior of such structures, allowing the detailed and efficient design of biomaterials that enable the controlled regulation of cell functionality.

Acknowledgements

This work was financially supported by the Helmholtz Association of German Research Centers through program-orientated funding and through Helmholtz Graduate School for Macromolecular Bioscience (MacroBio), grant no. VH-GS-503 (W. T.).

References

1. Muncie, J. M. & Weaver, V. M. The Physical and Biochemical Properties of the Extracellular Matrix Regulate Cell Fate. *Curr Top Dev Biol* **130**,1–37 (2018).

2. Yeung, T. *et al.* Effects of substrate stiffness on cell morphology, cytoskeletal structure, and adhesion. *Cell Motil Cytoskel* **60,** 24–34 (2005).

3. Chaudhuri, O. *et al.* Substrate stress relaxation regulates cell spreading. *Nat Commun* **6,** 6365 (2015).

4. Klein, E. A. *et al.* Cell-Cycle Control by Physiological Matrix Elasticity and In Vivo Tissue Stiffening. *Curr Biol* **19,** 1511–1518 (2009).

5. Hao, J. *et al.* Mechanobiology of mesenchymal stem cells: Perspective into mechanical induction of MSC fate. *Acta Biomater* **20,** 1–9 (2015).

6. Perestrelo, T., Correia, M., Ramalho-Santos, J. & Wirtz, D. Metabolic and Mechanical Cues Regulating Pluripotent Stem Cell Fate. *Trends*

Cell Biol **28,** 1014–1029 (2018).

7. Engler, A. J., Sen, S., Sweeney, L. H. & Discher, D. E. Matrix Elasticity Directs Stem Cell Lineage Specification. *Cell* **126,** 677–689 (2006).

8. Chaudhuri, O. *et al.* Hydrogels with tunable stress relaxation regulate stem cell fate and activity. *Nat Mater* **15**, 326-34 (2016).

9. Das, R. K., Gocheva, V., Hammink, R., Zouani, O. F. & Rowan, A. E. Stress-stiffening-mediated stem-cell commitment switch in soft responsive hydrogels. *Nat Mater* **15**, 318-25 (2016).

10. Frantz, C., ewart, K. & Weaver, V. M. The extracellular matrix at a glance. *J Cell Sci* **123,** 4195–4200 (2010).

11. Humphrey, J. D., Dufresne, E. R. & Schwartz, M. A. Mechanotransduction and extracellular matrix homeostasis. *Nat Rev Mol Cell Bio* **15,** 802–812 (2014).

12. Zündel, M., Ehret, A. E. & Mazza, E. The Multiscale Stiffness of Electrospun Substrates and Aspects of their Mechanical Biocompatibility. *Acta Biomater* **84,** 146–158 (2018).

13. Baker, B. M. *et al.* Cell-mediated fibre recruitment drives extracellular matrix mechanosensing in engineered fibrillar microenvironments. *Nature Mater* **14,** 1262–8 (2015).

14. Croisier, F. *et al.* Mechanical testing of electrospun PCL fibers. *Acta Biomater* **8,** 218–224 (2012).

15. Kumar, P. & Vasita, R. Understanding the relation between structural and mechanical properties of electrospun fiber mesh through uniaxial tensile testing. *J Appl Polym Sci* **134,** 26(2017).

16. Rizvi, Kumar, P., Katti, D. S. & Pal, A. Mathematical model of mechanical behavior of micro/nanofibrous materials designed for extracellular matrix substitutes. *Acta Biomater* **8,** 4111–4122 (2012).

17. Neugirg, B. R., Koebley, S. R., Schniepp, H. C. & Fery, A. AFM-

based mechanical characterization of single nanofibres. *Nanoscale* **8,** 8414–8426 (2016).

18. Chyasnavichyus, M., Young, S. L. & Tsukruk, V. V. Recent advances in micromechanical characterization of polymer, biomaterial, and cell surfaces with atomic force microscopy. *Jpn J Appl Phys* **54,** 08LA02 (2015).

19. Yang, L. *et al.* Mechanical properties of single electrospun collagen type I fibers. *Biomaterials* **29,** 955–962 (2008).

20. Kluge, D. *et al.* Influence of the Molecular Structure and Morphology of Self□Assembled 1,3,5□Benzenetrisamide Nanofibers on their Mechanical Properties. *Small* **8,** 2563–2570 (2012).

21. Kubow, K. E., Shuklis, V. D., Sales, D. J. & Horwitz, R. A. Contact guidance persists under myosin inhibition due to the local alignment of adhesions and individual protrusions. *Sci Rep-uk* **7**, 14380 (2017).

22. Cheng, X., Putz, K. W., Wood, C. D. & Brinson, C. L. Characterization of Local Elastic Modulus in Confined Polymer Films via AFM Indentation. *Macromol Rapid Comm* **36,** 391–397 (2015).

23. Kratz, K., Habermann, R., Becker, T., Richau, K. & Lendlein, A. Shape-memory properties and degradation behavior of multifunctional electro-spun scaffolds. *Int J Artif Organs* **34,** 225–230 (2011).

24. Fu, J. *et al.* Mechanical regulation of cell function with geometrically modulated elastomeric substrates. *Nat Methods* **7,** nmeth.1487 (2010).

25. Lv, H. *et al.* Mechanism of regulation of stem cell differentiation by matrix stiffness. *Stem Cell Res Ther* **6,** 1–11 (2015).

26. Geiger, B., Spatz, J. P. & Bershadsky, A. D. Environmental sensing through focal adhesions. *Nat Rev Mol Cell Bio* **10,** nrm2593 (2009).

27. Yan, J., Yao, M., Goult, B. T. & Sheetz, M. P. Talin Dependent Mechanosensitivity of Cell Focal Adhesions. *Cell Mol Bioeng* **8,** 151–159 (2015).

28. Yao, M. *et al.* The mechanical response of talin. *Nat Commun* **7,** 11966 (2016).

29. Hirata, H., Tatsumi, H., Lim, C. & Sokabe, M. Force-dependent vinculin binding to talin in live cells: a crucial step in anchoring the actin cytoskeleton to focal adhesions. *Am J Physiol-cell Ph* **306,** C607–C620 (2014).

30. Meacci, G. *et al.* α-Actinin links extracellular matrix rigidity-sensing contractile units with periodic cell-edge retractions. *Mol Biol Cell* **27,** 3471–3479 (2016).